Cross-layer Chase Combining with Selective Retransmission, Analysis and Throughput Optimization for OFDM Systems

Taniya Shafique, Zia Muhammad *Member, IEEE,* and Huy-Dung Han *Member, IEEE*

arXiv:1511.08290v1 [cs.IT] 26 Nov 2015

***Abstract*—In this paper, we present bandwidth efficient retransmission method employong selective retransmission approach at modulation layer under orthogonal frequency division multiplexing (OFDM) signaling. Our proposed cross-layer design embeds a selective retransmission sub-layer in physical layer (PHY) that targets retransmission of information symbols transmitted over poor quality OFDM sub-carriers. Most of the times, few errors in decoded bit stream result in packet failure at medium access control (MAC) layer. The unnecessary retransmission of good quality information symbols of a failed packet has detrimental effect on overall throughput of transceiver. We propose a cross-layer Chase combining with selective retransmission (CCSR) method by blending Chase combining at MAC layer and selective retransmission in PHY. The selective retransmission in PHY targets the poor quality information symbols prior to decoding, which results into lower hybrid automatic repeat reQuest (HARQ) retransmissions at MAC layer. We also present tight bit-error rate (BER) upper bound and tight throughput lower bound for CCSR method. In order to maximize throughput of the proposed method, we formulate optimization problem with respect to the amount of information to be retransmitted in selective retransmission. The simulation results demonstrate significant throughput gain of the proposed CCSR method as compared to conventional Chase combining method.**

Keywords: Hybrid ARQ, LDPC, throughput, OFDM, retransmission, cross-layer, LTE.

I. Introduction

The contemporary wireless communication standards such as LTE-advanced [1] integrate new technologies to meet increasing need of high data rate. The current and future communication systems employ multiple-input multiple-output (MIMO) technology due to its potential to achieve higher data rate and diversity. In order to assure error-free communication with high throughput over dynamic wireless channels, many packet error detection and correction protocols have evolved over time [2]. The automatic repeat reQuest (ARQ) methods combats packet loss that occurs due to channel fading of wireless networks and achieves error-free data transfer using cyclic redundancy check (CRC) approach. The concept of HARQ integrates ARQ and forward error correction (FEC) codes to provide effective means of enhancing overall throughput of communication systems [2], [3]. In the event of packet failure, an advanced form of HARQ incorporates joint decoding by combining soft information from multiple transmissions of a failed packet. Thus, HARQ is one of the most important technologies adopted in the latest communication standards such as high-speed down link packet access (HSDPA), universal mobile telecommunications system (UMTS) that pervade 3G and 4G wireless networks to ensure data reliability.

In type-I HARQ, the receiver requests retransmission of an erroneous packet and discards observation of the failed packet. Type-II HARQ is most commonly used method and achieves higher throughput. The type-II HARQ is divided into Chase combining HARQ (CC-HARQ) and incremental redundancy HARQ (IR-HARQ). In CC-HARQ, the receiver preserves observations of the failed packet and requests retransmission of full packet. The Chase receiver combines [4] observations of the failed packet and retransmitted packet for joint decoding. In the event of packet failure under IR-HARQ, the receiver requests retransmission of additional parity bits to recover from errors. In response to the retransmission request, transmitter sends more parity bits lowering the code rate of FEC code. After receiving requested parity bits, the receiver combines new parity bits with buffered observations for FEC joint decoding.

Most of the research conducted on HARQ focuses on ARQ and FEC [3], [5] without exploring the modulation layer. Throughput of capacity achieving FEC codes such as low density parity check (LDPC) codes and turbo codes is optimized for Rayleigh fading channel in [6] with ARQ and HARQ protocols. Mutual information based performance analysis of HARQ over Rayleigh fading channel is provided in [7]. Optimal power allocation for Chase combining based HARQ is optimized in [8]–[12]. Without exploiting channel state information and frequency diversity of the frequency selective channel, partial retransmission of the original symbol stream of a failed packet is addressed in [13]–[15]. These methods retransmit punctured packet in predetermined fashion without using channel knowledge. Furthermore, the complexity of joint detection for *partial* retransmission is

not tractable [13], [14], [16]. Partial retransmission of orthogonal space-time block (OSTB) coded [17] OFDM signaling is proposed in [15]. In [18], for conventional ARQ protocol, full packet retransmission at modulation layer is employed when channel gain is below a threshold value without buffering observations of low signal-to-noise ratio (SNR) channel realization.

In a typical failed packet, there are small number of corrupted bits and retransmission of full packet is not necessary. The receiver can recover from errors by retransmission of potentially culprit bits. The OFDM signaling allows to identify poor quality bits corresponding to the sub-carriers that have low SNR. Selective retransmission at modulation layer of OFDM signaling proposed in [19]–[22] achieves throughput gain as compared to conventional HARQ methods. However, throughput optimization of selective retransmission and performance analysis is not addressed in [19].

In LTE, two-levels packet retransmission achieves significant throughput gain and reduction in latency of the system. In the event of CRC failure, MAC sub-layer of user plane initiates retransmission request which results into low latency and higher throughput. The radio link control (RLC) sub-layer combats residual packet errors by ARQ retransmission [23], [24]. These retransmission schemes do not exploit channel state information (CSI). Most of the contemporary communication standards such as 3G and 4G network adopt OFDM modulation due to inherent robustness to combat multi-path effect of wireless channel and low complexity transceiver design [25]. In OFDM based systems, information symbols corresponding to the different coherence bandwidth encounter different channel gains. The motivation of selective retransmission owing to the fact that in the event of failed packet under OFDM signaling at MAC layer, often receiver can recover from error(s) by retransmitting *partial* information corresponding to the poor quality sub-carriers. An OFDM signaling allows selective retransmission of information symbols transmitted over poor quality sub-carrier at PHY level. After receiving the copy of information symbols corresponding to the poor quality sub-carriers, receiver jointly decodes data in Chase combining fashion. In this work, we propose a low complexity and bandwidth efficient CCSR cross-layer design at modulation layer for OFDM signaling. We also provide BER and throughput analysis in terms of tight upper BER bound and lower throughput bound, respectively, for the proposed retransmission scheme. The amount of information to be retransmitted for each sub-carrier in the event of failed packet is a function of signal-to-noise ratio (SNR) of the corresponding sub-carrier. In order to maximize throughput, we use norm of channel gain for each sub-carriers as channel quality measure and optimize threshold τ on channel norm for selective retransmission. The simulation results demonstrate that the proposed method offers substantial throughput gain as compared to the conventional CC method in low SNR regime. The results of proposed method show that there is marginal gap between analytical bounds and simulation results (Monte Carlo method) for both BER and throughput. The simulation results reveal that throughput gain of the proposed scheme also hold with LDPC FEC code.

We organize this manuscript as follows. First, we present the system model in Section II and problem formulation of CCSR method for OFDM system in Section III. In Section IV, we present BER analysis of the CCSR method in terms of BER upper bound. Throughput analysis for the proposed CCSR is presented in Section V. Throughput optimization is performed in Section VI. We discuss the results in Section VII. Finally, we conclude the proposed work in Section VIII.

II. SYSTEM MODEL

The system model under consideration employs three levels of retransmission as depicted in Figure 1. The two-layer ARQ approach in LTE achieves low latency and high throughput [1]. The system model in Figure 1 embeds an additional retransmission sub-layer in PHY for selective retransmission under OFDM modulation with N_s sub-carriers over frequency selective channel of L coefficients. An OFDM signaling converts frequency selective channel $\mathbf{h}$ into N_s parallel flat-fading channels [25]. The elements of a channel gain vector $H = \begin{bmatrix} H(1) & sH(\ell) & H(N_s) \end{bmatrix}^T$, where channel vector H is generated by applying Fourier transformation matrix $F \in \mathcal{C}^{N_s \times N_s}$ on frequency selective channel $\mathbf{h}$, are independent and identically distributed (i.i.d.) along time with distribution $\mathcal{N}(0,1)$ [25]. The matrix model of the received vector $\mathbf{y}$ over N_s sub-carriers can be written as

$$\mathbf{y} = \text{diag}(H)\mathbf{s} + \mathbf{w}, \tag{1}$$

where vector $\mathbf{w} \sim \mathcal{N}(0, N_0 I)$ is an additive white Gaussian noise vector. A typical failed packet has few erroneous bits. If we can identify unreliable bits, then full packet retransmission is unnecessary to recover failed packet. In OFDM modulation, information bits transmitted over sub-carriers with small channel norm $\|H(\ell)\|^2$ are more susceptible to the channel impairments. Thus, an OFDM signaling allows retransmission of targeted information symbols corresponding to the poor quality sub-carriers instead of unnecessary retransmission of full packet [19]. As shown in Figure 1, transmitter preserves information symbol vector $\mathbf{s} = [s(1) \ \ldots \ s(N_s)]^T$ and transmits OFDM modulated signal. The selective retransmission module of the receiver requests retransmission of information transmitted over the poor quality

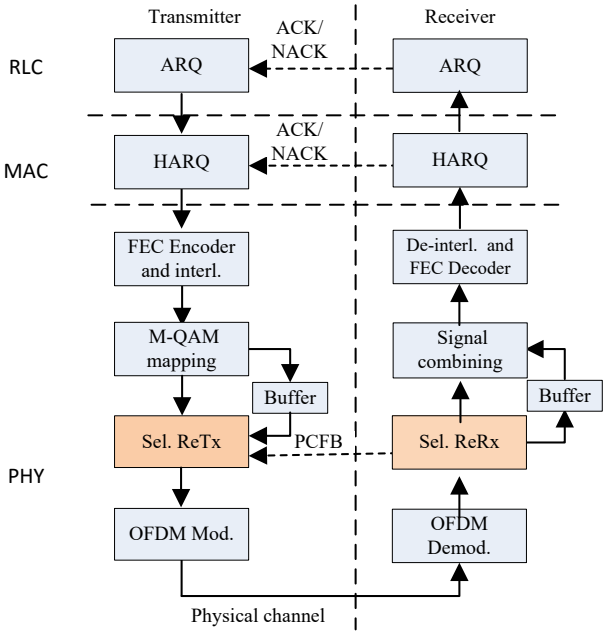

Fig. 1. Cross-layer system model for Chase combining with selective retransmission for OFDM system at PHY layer

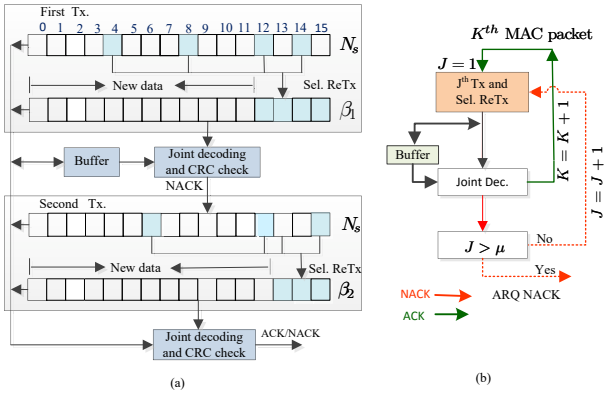

Fig. 2. (a) Chase combining with selective retransmission under OFDM signaling for two transmission rounds. (b) Flow graph of CCSR method for μ transmission rounds.

sub-carriers prior to decoding through partial channel feedback (PCFB). The norm of gain of a sub-carrier is measure of SNR of the sub-carriers. The receiver marks information symbols for selective retransmission corresponding to the sub-carriers, which have norm of gain below threshold τ. The threshold τ controls amount of information to be retransmitted discussed in Section IV. In response to the selective retransmission in PHY, peer selective retransmission module of the transmitter appends requested information symbols to the next OFDM symbol vector. Thus, each OFDM symbol vector consists of new information symbols and information symbols from the buffer in response to the selective retransmission request. The receiver then performs joint detection by combing observation of the first transmission and subsequent selective retransmission to enhance log-likelihood ratio (LLR) of bits for FEC decoding. Partial retransmission at modulation layer by targeting poor quality observations selectively improves BER and consequently lowers average number of retransmissions at MAC layer. HARQ layer delivers successfully decoded data units to the ARQ layer. When timeout for missing data unit occurs, ARQ layer request retransmission of corresponding packet from the peer ARQ layer of the transmitter. We propose CCSR selective retransmission method that achieves significant throughput gain as compared to the conventional CC-HARQ.

Note that retransmission of more information does not increase throughput linearly. The threshold parameter τ on the channel norm $\|H(\ell)\|^2$ of the ℓ-th sub-carriers controls amount of information to be retransmitted in selective retransmission with objective to maximize throughput of the communication system. We optimize threshold τ in order to maximize throughput η of the transceiver under selective retransmission. Throughput of selective retransmission is function of probability of error, which in fact is function of τ.

III. Problem Formulation

Now we present proposed cross-layer CCSR method for OFDM signaling. Similar to conventional HARQ, in CCSR method, MAC layer initiates retransmission in the event of CRC failure. The additional selective retransmission sub-layer in PHY layer initiates selective retransmission of information symbols transmitted over poor quality OFDM sub-carriers prior to decoding. Note that OFDM signaling allows retransmission of information symbols transmitted over poor quality sub-carriers ($\|H(\ell)\|^2 < \tau$) selectively avoiding overhead of retransmission of information symbols corresponding to good quality sub-carriers, where τ is threshold on channel norm of a sub-carrier. The receiver feeds back the partial channel state information (PCSI) when each coherent time is elapsed. We assume that due to longer retransmission delay, each retransmission encounters independent channel. Next, we present CCSR method under OFDM signaling.

The proposed CCSR method is depicted for $\mu = 2$ transmission rounds in Figure 2(a). Similar to conventional CC-HARQ method, MAC layer initiates full retransmission in the event of CRC failure. The proposed CCSR method is different from conventional CC-HARQ method in the sense that CCSR method employs an additional selective retransmission of information symbol corresponding to the poor quality sub-carriers at PHY

level for each transmission at MAC layer. For the first transmission of each MAC packet, proposed selective retransmission sub-layer initiates retransmission of the information symbols corresponding to the β_1 many sub-carriers which have $\|H_1(\ell)\|^2 < \tau$, where $H_1(\ell)$ represents gain of the ℓ-th sub-carrier corresponding to full transmission of the first round at MAC layer. For example, upper dotted rectangle of Figure 2(a) shows that OFDM sub-carriers 4, 8, 12 and 14 ($\beta_1 = 4$) have $\|H_1(\ell)\|^2 < \tau$ and are marked for retransmission, where ℓ is index to the sub-carrier. Selective retransmission sub-layer of the transmitter in response to the selective retransmission through feedback channel appends requested information symbols to the very next OFDM symbol. Note that for a very poor channel realizations, the proposed selective retransmission sub-layer in PHY may request retransmission of all information symbols ($\beta_1 = N_s$). Similarly, for good quality channel realizations, selective retransmission sub-layer can omit retransmission ($\beta_1 = 0$). On arrival of requested selective information, receiver performs joint detection and buffers $\beta_1 + N_s$ observations of first transmission and selective retransmission. Note that both transmitter and receiver keep track of information symbols which has been considered for selective retransmission in one transmission round. Each information symbol in one transmission round is consider only once for selective retransmission. With maximum transmission rounds μ at MAC layer, an information symbol can be considered at most μ times for selective retransmission at PHY level.

Let $H_{1s}(\ell)$ be the gain of the ℓ-th sub-carrier corresponding to the selective retransmission for the first transmission round, where subscript "s" stands for selective retransmission. Then the combined channel response $\mathcal{H}_1(\ell) = \left[H_1(\ell)\ H_{1s}(\ell)\right]^T$ for β_1 many sub-carriers is constructed by stacking channel of the first transmission and selective retransmission. If there are β_1 many sub-carriers with $\|H_1(\ell)\|^2 < \tau$, then there will be joint detection for β_1 sub-carrier for the first round of CCSR method. The estimate of $N_s - \beta_1$ information symbols which have sub-carrier gain $\|H_1(\ell)\|^2 \geq \tau$ after equalization is

$$\hat{s}(\ell) = s(\ell) + \frac{H_1^*(\ell)\mathbf{w}(\ell)}{\|H_1(\ell)\|^2} = s(\ell) + \mathbf{u}(\ell), \qquad (2)$$

where $\mathbf{u}(\ell)$ is the effective noise with distribution $\mathcal{N}(0, \|H(\ell)\|^{-2}N_0)$. Also the estimate of β_1 information symbols corresponding to the poor quality sub-carriers from the first full transmission as a result of joint detection is

$$\hat{s}(\ell) = s(\ell) + \underbrace{\|\mathcal{H}_1(\ell)\|^{-2}\mathcal{H}_1^H(\ell)\tilde{\mathbf{w}}(\ell)}_{\tilde{\mathbf{u}}(\ell)}, \qquad (3)$$

where $\tilde{\mathbf{u}}(\ell) \sim \mathcal{N}(0, \|\mathcal{H}_1(\ell)\|^{-2}N_0I_2)$ and $\tilde{\mathbf{w}}(\ell) \sim \mathcal{N}(0, N_0I_2)$. Note that MAC layer is unaware of selective retransmission sub-layer in PHY. The selective retransmission followed by joint detection at modulation layer enhances reliability of the decoded bits resulting into few CRC failure at MAC layer by selectively retransmitting poor quality information symbols.

In the event of CRC failure, MAC layer initiates next round of HARQ retransmission by sending NACK signal to the peer MAC layer for the full retransmission of failed data as shown in the lower dotted rectangle of the Figure 2(a). In response to NACK from MAC layer, transmitter retransmits failed full packet similar to conventional CC-HARQ as shown in Figure 2(a). Similar to the first transmission, selective retransmission sub-layer initiates selective retransmission of poor quality symbols of retransmitted full packet from MAC layer. As a result of selective retransmission, transmitter appends β_2 many ($\beta_2 = 3$ in Figure 2(a)) information symbols to the next immediate OFDM symbol. When selective retransmission is employed in PHY, Chase combining processes $2N_s + \beta_1 + \beta_2$ observations instead of $2N_s$ observations for joint detection. Note that $E[\beta_1] = E[\beta_2] = N_sP(\|H_1(\ell)\|^2 < \tau) = N_sP(\|H_{1s}(\ell)\|^2 < \tau) = N_sm$, where $H_{1s}(\ell)$ is channel gain of the ℓ-th sub-carrier during selective retransmission.

Let μ be the maximum number of allowed retransmission of a MAC packet and J be the round counter for the transmission of the k-th MAC packet of a HARQ process for CCSR method. At the end of the J-th round, where $J = 1, \ldots, \mu$, receiver combines buffered observations of full transmissions and selective retransmissions of J rounds for joint detection. If CRC fails after μ rounds of MAC layer, receiver clears observations from the buffer and sends signal to the ARQ layer. In response to the packet failure, ARQ layer initiates new retransmission round by initiating retransmission request to the peer ARQ layer. The flow graph of CCSR protocol for the k-th MAC packet is presented in Figure 2(b) and described in Algorithm 1. If CRC failure occurs after μ MAC retransmissions, retransmission of failed packet is initiated from ARQ layer. The algorithm of CCSR method is described as follows:

IV. Performance Analysis

In this section, we present tight upper bounds on BER of joint detection after signal combining and prior to channel decoding for cross-layer CCSR method. One round of transmission of CCSR method includes one full transmission of MAC packet followed by selective retransmission of information symbols corresponding to the sub-carriers which have $\|H(\ell)\|^2 < \tau$, where $H(\ell)$ is gain of ℓ-th sub-carrier. We assume that full transmission by MAC layer and subsequent selective retransmission

Algorithm 1 CCSR protocol

1: $J = 1$ corresponds to the first transmission of the k-th MAC packet
2: Selective retransmission of β_J sub-carriers and buffering of N_s observations
3: Joint decoding from $JN_s + \sum_{i=1}^{J} \beta_i$ observations and CRC check
4: **if** CRC satisfies **then** $k = k+1$, discard observations and go to 1
5: **if** $J \geq \mu$ **then** declare packet loss, discard observation, ARQ sub-layer initiates NACK for retransmission of packet and go to 1
6: $J = J + 1$ and go to 2

by PHY layer encounter independent channel realizations. In this analysis, we consider maximum of μ transmission rounds at MAC layer. Similar to conventional Chase combining, joint detection for the J-th round combines observations buffered up to J rounds. Thus, probability of error P_{e_J} of the joint detection of the J-th round is lower than that of $J-1$-th round ($P_{e_J} < P_{e_{J-1}}$), where $J \leq \mu \in I^+$. In order to evaluate throughput of the proposed CCSR method in Section V, we derive closed form expression for the upper bound on BER of joint detection of J-th round under maximum number of μ transmission rounds of a MAC packet. Now we evaluate P_{e_J} for the J-th round.

A. BER analysis of the first round of CCSR

Let H_1 and H_{1s} be the complex gain vectors of length N_s corresponding to the full transmission by MAC layer and subsequent selective retransmission from PHY layer, respectively. Each element $H_1(\ell)$ and $H_{1s}(\ell)$ of the complex channel gain vectors of OFDM sub-carriers follows Gaussian distribution with zero-mean and unit variance [25]. One MAC data unit is mapped to N_s information symbols using M-QAM modulation, where N_s is the number of sub-carriers of an OFDM symbol. Prior to decoding, selective retransmission sub-layer initiates selective retransmission of β_1 poor quality information symbols as shown in upper dotted rectangle of Figure 2(a). We denote the outcomes $\|H_1(\ell)\|^2 \geq \tau$ and $\|H_1(\ell)\|^2 < \tau$ of the first full transmission by the events ξ and ξ^c, respectively. The probabilities of events ξ and ξ^c are $P(\xi^c) = P(\|H_1(\ell)\|^2 < \tau)$ and $P(\xi) = P(\|H_1(\ell)\|^2 \geq \tau)$, respectively, where random variable $\chi_1 = \|H_1(\ell)\|^2$ has chi-square distribution of degree 2 [26] and $P(\xi^c) = 1 - P(\xi) = P(\chi_1 < \tau)$. For Rayleigh fading channel, real and imaginary components of complex channel coefficient of a sub-carrier have zero-mean and variance $\sigma^2 = \frac{1}{2}$. When event ξ occurs, selective retransmission sub-layer omits retransmission of that particular sub-carriers.

When event ξ^c occurs for ℓ-th sub-carrier, selective retransmission sub-layer request retransmission of that very information symbol $s(\ell)$ and receiver performs joint detection by combining observation of the full transmission and subsequent selective retransmission. Note that the random variable $\|\mathcal{H}_1(\ell)\|^2$ in (3) also has chi-square distribution of degree 4. Also that $\|\mathcal{H}_1(\ell)\|^2 = \chi_1 + \chi_2$, where chi-square random variables χ_1 and $\chi_2 = \|H_{1s}(\ell)\|^2$ are i.i.d. of degree 2 each. The bit-error probability of joint detection for selective retransmission over Rayleigh fading channel is

$$P_{e_1} = E_H\Big[P(\xi)\ \ P_{e|\xi} + P(\xi^c)\ \ P_{e|\xi^c}\Big], \tag{4}$$

where $P_{e|\xi}$ and $P_{e|\xi^c}$ are the conditional bit-error probabilities of detection from single observation and joint detection, respectively.

The probability of error for joint detection of first round of CCSR is

$$P_{e_1} = P(\xi)cE_{H|\xi}\left[Q\left(\sqrt{g\frac{\chi_1}{N_0}}\right)\right] + P(\xi^c)cE_{\mathcal{H}|\xi^c} \left[Q\left(\sqrt{g\frac{\chi_1+\chi_2}{N_0}}\right)\right], \tag{5}$$

where $E_{H|\xi^c}$ and $E_{\mathcal{H}|\xi}$ are conditional expectations. Also, c and g are modulation constants [25]. The conditional probability density function $f_{\chi_1|\xi^c}(x_1)$ of $f_{\chi_1}(x_1)$ when $\chi_1 \geq \tau$ is $f_{\chi_1|\xi^c}(x_1) = \dfrac{f_{\chi_1}(x_1)}{P(\xi^c)}$. In order to solve first term of (5), we have [27]

$$E_{H|\xi}\left[Q\left(\sqrt{g\frac{\chi_1}{N_0}}\right)\right] = \int_{\tau}^{\infty} Q\left(\sqrt{g\frac{x_1}{N_0}}\right)\frac{f_{\chi_1}(x_1)}{P(\xi)}dx_1 \tag{6}$$

Similarly,

$$E_{H|\xi^c}\left[Q\left(\sqrt{g\frac{\chi_1+\chi_2}{N_0}}\right)\right] = \int_{x_1=0}^{\tau}\int_{x_2=0}^{\infty} Q\left(\sqrt{g\frac{x_1+x_2}{N_0}}\right) \frac{f_{\chi_1}(x_1)f_{\chi_2}(x_2)}{P(\xi^c)}dx_2dx_1 \tag{7}$$

The upper bound on P_{e_1} in (5) using approximation of Q-function [28], (6) and (7) can be written as [22], [27]

$$P_{e_1} \leq \frac{c}{12}\int_{\tau}^{\infty}\exp(-g\frac{x_1}{2N_0})f_{\chi_1}(x_1)dx_1 + \frac{c}{4}\int_{\tau}^{\infty} \exp(-g\frac{4x_1}{3.2N_0})f_{\chi_1}(x_1)dx_1 + \frac{c}{12}\int_{0}^{\tau}\exp(-g\frac{x_1}{2N_0})f_{\chi_1}(x_1) dx_1\int_{0}^{\infty}\exp(-g\frac{x_2}{2N_0})f_{\chi_2}(x_2)dx_2 + \frac{c}{4}\int_{0}^{\tau}\exp(-g\frac{4x_1}{3.2N_0}) f_{\chi_1}(x_1)dx_1\int_{0}^{\infty}\exp(-g\frac{4x_2}{3.2N_0})f_{\chi_2}(x_2)dx_2, \tag{8}$$

Note that $\rho = \sqrt{\frac{\sigma^2 N_o}{g\sigma^2+N_o}}$, $\rho_1 = \sqrt{\frac{\sigma^2 N_o}{g_1\sigma^2+N_o}}$ and $g_1 = \frac{4g}{3}$. For 4-QAM constellation $g = 2$ and $c = \frac{2}{\log_2 M}$. By

simplifying (8), we have upper bound on probability of error of the joint detection of the first round as follows [26]

$$P_{e_1} \leq \frac{c}{12}\left(\frac{\rho}{\sigma}\right)^2 \exp\left(-\frac{\tau}{2\rho^2}\right) + \frac{c}{4}\left(\frac{\rho_1}{\sigma}\right)^2 \exp\left(-\frac{\tau}{2\rho_1^2}\right) + \frac{c}{12}\left(\frac{\rho}{\sigma}\right)^4 \left(1-\exp\left(-\frac{\tau}{2\rho^2}\right)\right) + \frac{c}{4}\left(\frac{\rho_1}{\sigma}\right)^4 \left(1-\exp\left(-\frac{\tau}{2\rho_1^2}\right)\right). \quad (9)$$

Now we evaluate BER upper bound of joint detection for second round under CCSR method.

B. BER analysis of second round of CCSR

Let $H_2(\ell)$ be the gain of the ℓ-th sub-carrier corresponding to the full retransmission initiated from the MAC layer as a result of CRC failure of MAC packet of the first round and $H_{2s}(\ell)$ be the channel gain for selective retransmission. In a similar fashion to the first round, the receiver marks data symbol of the second round transmitted over ℓ-th sub-carrier for selective retransmission for the second round if $\|H_2\|^2 < \tau$. The channel gains $H_1(\ell)$ and $H_2(\ell)$ of the full transmission of the first and second round, respectively, of the ℓ-th sub-carrier are independent, which results into four possible joint channel vectors for joint detection. We denote each possible outcome of joint channel vector by an event. The probability of error of joint detection of the second round is

$$P_{e_2} = E_H\big[P(\xi_1)P_{e|\xi_1} + P(\xi_2)P_{e|\xi_2} + P(\xi_3)P_{e|\xi_3} + P(\xi_4)P_{e|\xi_4}\big], \quad (10)$$

where events $\xi_1,\ \xi_2, \xi_3$ and ξ_4 correspond to the four joint channel vectors defined as follows:

1) Event ξ_1 occurs when $\|H_1(\ell)\|^2 \geq \tau$ and $\|H_2(\ell)\|^2 \geq \tau$ for the first and second full transmissions, respectively. The resulting joint channel for joint detection of CCSR is $\mathcal{H}_1(\ell) = [H_1(\ell)\ \ H_2(\ell)]^T$, where $H_1(\ell)$ and $H_2(\ell)$ are i.i.d. channel realizations with Gaussian distribution of zero-mean and unit variance. The channel norm $\|\mathcal{H}_1(\ell)\|^2 = \|H_1(\ell)\|^2 + \|H_2(\ell)\|^2$ has chi-square distribution.
2) Event ξ_2 occurs when $\|H_1(\ell)\|^2 < \tau$ and $\|H_2(\ell)\|^2 \geq \tau$. The resulting joint channel response for joint detection of CCSR is $\mathcal{H}_2(\ell) = [H_1(\ell)\ \ H_{1s}(\ell)\ \ H_2(\ell)]^T$.
3) Event ξ_3 occurs when $\|H_1(\ell)\|^2 \geq \tau$ and $\|H_2(\ell)\|^2 < \tau$. The resulting joint channel response for joint detection of CCSR is $\mathcal{H}_3(\ell) = [H_1(\ell)\ \ H_2(\ell)\ \ H_{2s}(\ell)]^T$, where $H_{2s}(\ell)$ is channel gain of the ℓ-th sub-carrier selected for retransmission during selective retransmission of the second round of packet at MAC layer.
4) Event ξ_4 occurs when $\|H_1(\ell)\|^2 < \tau$ and $\|H_2(\ell)\|^2 < \tau$. The resulting joint channel for joint detection of CCSR is $\mathcal{H}_4(\ell) = [H_1(\ell)\ \ H_{1s}(\ell)\ \ H_2(\ell)\ \ H_{2s}(\ell)]^T$, where $H_{1s}(\ell)$ and $H_{2s}(\ell)$ are the channels corresponding to the selective retransmissions of the first round and second round, respectively. Note that random variables $\|H_{1s}(\ell)\|^2$ and $\|H_{2s}(\ell)\|^2$ are also i.i.d. with chi-square distribution of degree 2 each.

The second and third terms in (10) are equivalent due to the fact that $P(\xi_2) = P(\xi_3)$ and random variables $\|\mathcal{H}_2(\ell)\|$ and $\|\mathcal{H}_3(\ell)\|$ are i.i.d. Therefore, $E_H\Big[P(\xi_2)P_{e|\xi_2} + P(\xi_3)P_{e|\xi_3}\Big] = 2E_H\Big[P(\xi_2)P_{e|\xi_2}\Big]$. Note that all channel realizations of the ℓ-th sub-carrier of an OFDM system are i.i.d. with Gaussian distribution of zero-mean and unit variance. In order to achieve upper bound on BER for joint detection of CCSR method, we rewrite (10) as follows:

$$P_{e_2} = cE_H\left[P(\xi_1)Q\left(\sqrt{\frac{g\|\mathcal{H}_1(\ell)\|^2}{N_0}}\right) + 2P(\xi_2)Q\left(\sqrt{\frac{g\|\mathcal{H}_2(\ell)\|^2}{N_0}}\right) + P(\xi_4)Q\left(\sqrt{\frac{g\|\mathcal{H}_4(\ell)\|^2}{N_0}}\right)\right]. \quad (11)$$

Note that $\|\mathcal{H}_1(\ell)\|^2 = \chi_1 + \chi_2$ in the first term of (11) is sum if two i.i.d. chi-square random variables , where $\chi_1 \geq \tau$ and $\chi_2 \geq \tau$. Using approximation of Q-function in [28] and, following (6) and (7), we have

$$\begin{aligned} E_H\left[P(\xi_1)P_e|\xi_1\right] &= cE_H\left[P(\xi_1)Q\left(\sqrt{\frac{g\|\mathcal{H}_1(\ell)\|^2|\xi_1}{N_0}}\right)\right] \\ &\leq \frac{c}{12}\int_\tau^\infty \exp(-g\frac{x_1}{2N_0})f_{\chi_1}(x_1)dx_1 \int_\tau^\infty \exp(-g\frac{x_2}{2N_0}) f_{\chi_2}(x_2)dx_2 + \frac{c}{4}\int_\tau^\infty \exp(-g\frac{4x_1}{3.2N_0})f_{\chi_1}(x_1)dx_1 \int_\tau^\infty \exp(-g\frac{4x_2}{3.2N_0})f_{\chi_2}(x_2)dx_2 \\ &= \frac{c}{12}\left(\frac{\rho}{\sigma}\right)^4\left(\exp\left(-\frac{\tau}{2\rho^2}\right)\right)^2 + \frac{c}{4}\left(\frac{\rho_1}{\sigma}\right)^4\left(\exp\left(-\frac{\tau}{2\rho_1^2}\right)\right)^2. \end{aligned} \quad (12)$$

Similarly,

$$E_H\left[P(\xi_2)P_e|\xi_2\right]=cE_H\left[P(\xi_2)Q\left(\sqrt{\frac{g\|\mathcal{H}_2(\ell)\|^2|\xi_2}{N_0}}\right)\right]$$
$$\leq \frac{c}{12}\int_0^{\tau}\exp(-g\frac{x_1}{2N_0})f_{\chi_1}(x_1)dx_1\int_0^{\infty}\exp(-g\frac{x_{1s}}{2N_0})$$
$$f_{\chi_{1s}}(x_{1s})dx_{1s}\int_{\tau}^{\infty}\exp(-g\frac{x_2}{2N_0})f_{\chi_2}(x_2)dx_2+$$
$$\frac{c}{4}\int_0^{\tau}\exp(-g\frac{4x_1}{3.2N_0})f_{\chi_1}(x_1)dx_1\int_0^{\infty}\exp(-g\frac{4x_{1s}}{3.2N_0})$$
$$f_{\chi_{1s}}(x_{1s})dx_{1s}\int_{\tau}^{\infty}\exp(-g\frac{4x_2}{3.2N_0})f_{\chi_2}(x_2)dx_2, \quad (13)$$

where $\chi_1<\tau$, $\chi_{1s}\in\mathcal{R}$ and $\chi_2\geq\tau$. Simplifying (13), we have

$$E_H\left[P(\xi_2)P_e|\xi_2\right]\leq\frac{c}{12}\left(\frac{\rho}{\sigma}\right)^6\left(1-\exp\left(-\frac{\tau}{2\rho^2}\right)\right)$$
$$\left(\exp\left(-\frac{\tau}{2\rho^2}\right)\right)+\frac{c}{4}\left(\frac{\rho_1}{\sigma}\right)^6\left(1-\exp\left(-\frac{\tau}{2\rho_1^2}\right)\right)$$
$$\left(\exp\left(-\frac{\tau}{2\rho_1^2}\right)\right). \quad (14)$$

Also, it can be shown that

$$E_H\left[P(\xi_4)P_e|\xi_4\right]=cE_H\left[P(\xi_4)Q\left(\sqrt{\frac{g\|\mathcal{H}_4(\ell)\|^2|\xi_4}{N_0}}\right)\right]$$
$$\leq\frac{c}{12}\Big(\frac{\rho}{\sigma}\Big)^8\left(1-\exp\Big(-\frac{\tau}{2\rho^2}\Big)\right)^2+\frac{c}{4}\Big(\frac{\rho_1}{\sigma}\Big)^8$$
$$\left(1-\exp\Big(-\frac{\tau}{2\rho_1^2}\Big)\right)^2, \quad (15)$$

where $\chi_1<\tau$, $\chi_{1s}\in\mathcal{R}$, $\chi_2<\tau$ and $\chi_{2s}\in\mathcal{R}$. Now using (12), (14) and (15) in (11), we have

$$P_{e_2}\leq\frac{c}{12}\Big(\frac{\rho}{\sigma}\Big)^4\left(\exp\Big(-\frac{\tau}{2\rho^2}\Big)\right)^2+\frac{c}{4}\Big(\frac{\rho_1}{\sigma}\Big)^4$$
$$\left(\exp\Big(-\frac{\tau}{2\rho_1^2}\Big)\right)^2+\frac{c}{6}\Big(\frac{\rho}{\sigma}\Big)^6\left(\exp\Big(-\frac{\tau}{2\rho^2}\Big)\right)$$
$$\left(1-\exp\Big(-\frac{\tau}{2\rho^2}\Big)\right)+\frac{c}{2}\Big(\frac{\rho_1}{\sigma}\Big)^6\left(\exp\Big(-\frac{\tau}{2\rho_1^2}\Big)\right)$$
$$\left(1-\exp\Big(-\frac{\tau}{2\rho_1^2}\Big)\right)+\frac{c}{12}\Big(\frac{\rho}{\sigma}\Big)^8\left(1-\exp\Big(-\frac{\tau}{2\rho^2}\Big)\right)^2$$
$$+\frac{c}{4}\Big(\frac{\rho_1}{\sigma}\Big)^8\left(1-\exp\Big(-\frac{\tau}{2\rho_1^2}\Big)\right)^2. \quad (16)$$

The following proposition generalizes BER upper bound on joint detection for J transmission rounds:

Proposition 1. *The upper bound on BER for joint decoding of J transmission rounds under selective retransmissions is*

$$P_{e_J}=\sum_{i=0}^{J}\left\{\binom{J}{i}\frac{c}{12}\left(\frac{\rho}{\sigma}\right)^{2(J+i)}\left(\exp\left(-\frac{\tau}{2\rho^2}\right)\right)^{(J-i)}\right.$$
$$\left(1-\exp\left(-\frac{\tau}{2\rho^2}\right)\right)^i+\binom{J}{i}\frac{c}{4}\left(\frac{\rho_1}{\sigma}\right)^{2(J+i)}$$
$$\left.\left(\exp\left(-\frac{\tau}{2\rho_1^2}\right)\right)^{(J-i)}\left(1-\exp\left(-\frac{\tau}{2\rho_1^2}\right)\right)^i\right\}. \quad (17)$$

Proof: For J transmission rounds, there are 2^J possible joint detection channel vectors and we define $J+1$ events. The event ξ_i consists of $\binom{J}{i}$ joint channel vectors. Each joint vector includes channel gains from the full transmissions and selective retransmissions. Note that when channel gain of the ℓ-th sub-carrier of the full transmission of each round has $\|H_j\|^2\geq\tau$, where $j=1,\ldots,J$, the size of joint channel vector is J. The event ξ_i occurs when i sub-carrier realizations out of J realizations of the ℓ-th sub-carriers corresponding to the full transmissions have $\|H_j(\ell)\|^2<\tau$ in any order. Thus, there are $\binom{J}{i}$ joint channel vector realizations out of 2^J possible outcomes which have i sub-carrier gains below threshold τ in any order for the joint detection of the J-th round. For example, for joint detection of 4 round of CCSR ($J=4$) and $i=2$, there are 2 channel gains out of 4 for which channel-norm is lower than τ in any order. The possible $\binom{4}{2}=6$ many joint channel gain vectors belong to the event ξ_2 are

$$\xi_2=\{[H_1(\ell)\ \ H_{1s}(\ell)\ \ H_2(\ell)\ \ H_{2s}(\ell)\ \ H_3(\ell)\ \ H_4(\ell)]^T,$$
$$[H_1(\ell)\ \ H_{1s}(\ell)\ \ H_2(\ell)\ \ H_3(\ell)\ \ H_{3s}(\ell)\ \ H_4(\ell)]^T,$$
$$[H_1(\ell)\ \ H_{1s}(\ell)\ \ H_2(\ell)\ \ H_3(\ell)\ \ H_4(\ell)\ \ H_{4s}(\ell)]^T,$$
$$[H_1(\ell)\ \ H_2(\ell)\ \ H_{2s}(\ell)\ \ H_3(\ell)\ \ H_{3s}(\ell)\ \ H_4(\ell)]^T,$$
$$[H_1(\ell)\ \ H_2(\ell)\ \ H_{2s}(\ell)\ \ H_3(\ell)\ \ H_4(\ell)\ \ H_{4s}(\ell)]^T,$$
$$[H_1(\ell)\ \ H_2(\ell)\ \ H_3(\ell)\ \ H_{3s}(\ell)\ \ H_4(\ell)\ \ H_{4s}(\ell)]^T\}.$$

The elements of joint sub-carrier gain vectors are independent with Gaussian distribution of zero-mean and variance $\sigma^2=\frac{1}{2}$. All the 6 joint channel vectors have equal impact on BER and are equivalent. Therefore, without loss of generality, all 6 channel gain vectors of event ξ_2 can be represented by a single joint channel vector

$$\mathcal{H}_2=[H_1(\ell)\ \ H_2(\ell)\ \ H_3(\ell)\ \ H_4(\ell)\ \ H_{1s}(\ell)\ \ H_{2s}(\ell)\ \ ]^T.$$

The joint gain vector, which represents all joint channels of the event ξ_i of the J-th round can be written as

$$\mathcal{H}_i = \Bigg[\underbrace{H_1(\ell)\dots H_i(\ell)}_{\|H_j(\ell)\|^2<\tau} \underbrace{H_{i+1}(\ell)\ \dots\ H_J(\ell)}_{\|H_j(\ell)\|^2\geq\tau} H_{1s}(\ell)\dots\ H_{is}(\ell) \Bigg]^T,$$

and probability of occurring event ξ_i is $P(\xi_i) = p_1^{(J-i)} p_2^i \binom{J}{i}$, where $P(\|H_j(\ell)\|^2 \geq \tau) = P(\xi) = p_1$ and $P(\|H_j(\ell)\|^2 < \tau) = P(\xi^c) = p_2$. Note that i gains of $\mathcal{H}_i$ have $\|H_j\|^2 < \tau$, where $j = 1, \dots,\ i$ and $J-i$ gains of joint channel $\mathcal{H}_i$ have $\|H_j\|^2 \geq \tau$, where $j = i+1, \dots,\ J$. The event ξ_0 has all channel gains with $\|H_j\|^2 \geq \tau$ and event ξ_J has all channel gains with $\|H_j\|^2 < \tau$. Furthermore, all elements of vector $\mathcal{H}_i$ have chi-square distribution of order 2. The probability of error of joint detection of the J-th round is

$$P_{e_J} = E_H\Big[\sum_{i=0}^{J} P(\xi_i) P_{e|\xi_i}\Big] = \sum_{i=0}^{J} E_H\big[P(\xi_i) P_{e|\xi_i}\big]. \tag{18}$$

Now we evaluate $E_H\Big[P(\xi_i)P_{e|\xi_i}\Big]$ as follows:

$$\begin{aligned}
&E_H\left[P(\xi_i)P_{eJ}|\xi_i\right] = cE_H\left[P(\xi_i)Q\left(\sqrt{\frac{g\|\mathcal{H}_i(\ell)\|^2|\xi_i}{N_0}}\right)\right] \\
&\leq \binom{J}{i}\frac{c}{12}\prod_{k=1}^{J-i}\int_{\tau}^{\infty}\exp(-g\frac{x_k}{2N_0})f_{\chi_k}(x_k)dx_k \prod_{k=J-i+1}^{J}\int_0^{\tau}\exp(-g\frac{x_k}{2N_0})f_{\chi_k}(x_k)dx_k \\
&\prod_{k=1}^{i}\int_0^{\infty}\exp(-g\frac{x_{ks}}{2N_0})f_{\chi_{ks}}(x_{ks})dx_{ks} + \binom{J}{i}\frac{c}{4}\prod_{k=1}^{J-i}\int_{\tau}^{\infty}\exp(-g\frac{4x_k}{3.2N_0}) \\
&f_{\chi_k}(x_k)dx_k \prod_{k=J-i+1}^{J}\int_0^{\tau}\exp(-g\frac{4x_k}{3.2N_0})f_{\chi_k}(x_k)dx_k \\
&\prod_{k=1}^{i}\int_0^{\infty}\exp(-g\frac{4x_{ks}}{3.2N_0})f_{\chi_{ks}}(x_{ks})dx_{ks} \\
&= \frac{c}{12}\binom{J}{i}\left(\frac{\rho}{\sigma}\right)^{2(J+i)}\left(\exp\left(-\frac{\tau}{2\rho^2}\right)\right)^{(J-i)} \\
&\left(1-\exp\left(-\frac{\tau}{2\rho^2}\right)\right)^{i} + \frac{c}{4}\binom{J}{i}\left(\frac{\rho_1}{\sigma}\right)^{2(J+i)} \\
&\left(\exp\left(-\frac{\tau}{2\rho_1^2}\right)\right)^{(J-i)}\left(1-\exp\left(-\frac{\tau}{2\rho_1^2}\right)\right)^{i}.
\end{aligned} \tag{19}$$

Now by substituting $E_H\big[P(\xi_i)P_{e|\xi_i}\big]$ in (18), we have

$$\begin{aligned}
P_{e_J} &= \sum_{i=0}^{J}\binom{J}{i}\frac{c}{12}\left(\frac{\rho}{\sigma}\right)^{2(J+i)}\left(\exp\left(-\frac{\tau}{2\rho^2}\right)\right)^{(J-i)} \\
&\left(1-\exp\left(-\frac{\tau}{2\rho^2}\right)\right)^{i} + \binom{J}{i}\frac{c}{4}\left(\frac{\rho_1}{\sigma}\right)^{2(J+i)} \\
&\left(\exp\left(-\frac{\tau}{2\rho_1^2}\right)\right)^{(J-i)}\left(1-\exp\left(-\frac{\tau}{2\rho_1^2}\right)\right)^{i}.
\end{aligned} \tag{20}$$

■

In order to compute probability for error of the proposed CCSR method with μ (maximum allowed MAC retransmissions), we consider (20) with highest possible $J = \mu$, where $J = 1, 2, \dots, \mu$.

In next section, we present throughput analysis and optimization with respect parameter τ for CCSR for μ MAC retransmissions (rounds).

V. Throughput Analysis

Now we present throughput analysis of the proposed CCSR method. In throughput analysis, we consider non-truncated ARQ which has infinite many retransmission rounds. There are μ retransmissions rounds of a HARQ process at MAC layer in one ARQ round as depicted in Figure 2. One retransmission round of HARQ process consists of a full transmission of HARQ packet followed by a selective retransmission in PHY. In practice, transceiver pair continues retransmission rounds until error-free packet is received or maximum number of retransmission rounds are reached. For throughput analysis, we follow conventional definition of throughput η, which is the ratio of error-free information bits received k to the total number of bits transmitted n ($\eta = \frac{k}{n}$). Note that P_{e_J} is the bit-error probability of the joint detection of the J-th round of MAC transmission given in (20). Assuming that each bit in the frame is independent, probability of receiving an error-free packet of length L_f with probability of bit-error P_{e_J} is $p_{c_J} = (1-P_{e_J})^{L_f}$. The probability of receiving a bad packet is $p_{\epsilon_J} = 1 - p_{c_J}$. As a direct consequence of joint detection, probability of bit-error $P_{e_1} > P_{e_2} > \ldots > P_{e_\mu}$ and probability of receiving correct packet $p_{c_1} < p_{c_2} < \ldots < p_{c_\mu}$.

One transmission round of HARQ layer consists of k information bits of the full transmission and mk bits of selective retransmission, where $m = p_2 = P(\|H_1(\ell)\|^2 < \tau)$. Thus, there are $I = k(1+m)$ bits transmitted in one transmission round of MAC layer to the receiver. As a result of joint detection, $P_{e_J} < P_{e_{J-1}}$, $p_{c_J} > p_{c_{J-1}}$ and $p_{\epsilon_J} < p_{\epsilon_{J-1}}$. The probability that a packet fails after two transmission is $p_{\epsilon_1}p_{\epsilon_2}$. Note that if CRC failure occurs after μ transmissions at MAC layer, receiver discards observations of μ transmissions and

ARQ layer initiates a new round of transmission of the failed packet. Thus probability of CRC failure at the end of μ transmissions is $\alpha = \prod_{j=1}^{\mu} p_{\epsilon_j} = p_{\epsilon_1}.p_{\epsilon_2}\dots p_{\epsilon_\mu}$. The probability of a packet to fail after q transmissions with joint detection of μ transmissions at MAC layer is

$$p_{\epsilon_q} = \big(p_{\epsilon_1}.p_{\epsilon_2}\dots p_{\epsilon_\mu}\big)^{\gamma}\prod_{j=1}^{J} p_{\epsilon_{J-j}} = \alpha^{\gamma}\prod_{j=1}^{J} p_{\epsilon_{J-j}} \quad (21)$$

where $\gamma = \lfloor\frac{q-1}{\mu}\rfloor$, $J = [(q-1) \mod \mu] + 1$ and $p_{\epsilon_0} = 1$. Note that $\gamma = 0, 1, \dots, \infty$, $J = 1, 2, \dots, \mu$ represent transmission count at MAC layer. Since there is joint detection of at most μ packets and observations are discarded in the event of successful decoding or failure of every μ-th packet, the probability receiving error-free packet in the event of $\mu+1$-th transmission of a packet is p_{c_1}. The probability of successful decoding of q-th transmission of a failed packet is p_{c_J}.

The number of bits transmitted in q transmissions of a packet is $k(1+m)q$. The average number of bits that transmitter transmits n_μ for successful decoding of a packet in given channel condition with μ transmission rounds at MAC layer in one ARQ round is stated as follows:

Proposition 2. *The expected number of information bits under maximum number of μ rounds at MAC layer and non-truncated retransmissions at ARQ layer is sum of μ summation series as*

$$n_\mu = \sum_{J=1}^{\mu} n_{J,\mu}, \quad (22)$$

where

$$n_{J,\mu} = Jb_J + (J+\mu)b_J\alpha + (J+2\mu)b_J\alpha^2 + (J+3\mu)b_J\alpha^3 + \dots, \quad (23)$$

$\alpha = \prod_{j=1}^{\mu} p_{\epsilon_j}$, $b_J = Ip_{\epsilon_1}p_{\epsilon_2}\dots p_{\epsilon_{J-1}}p_{c_J} = k(1+m)\prod_{j=1}^{J} p_{\epsilon_{J-j}}p_{c_J}$ *and* $p_{\epsilon_0} = 1$.

Proof: The expected number of information bits transmitted to deliver error-free k information bits for the proposed CCSR method are [29]

$$\begin{aligned} n_\mu = {} & Ip_{c_1} + 2Ip_{\epsilon_1}p_{c_2} + 3Ip_{\epsilon_1}p_{\epsilon_2}p_{c_3} + \dots + \mu Ip_{\epsilon_1}p_{\epsilon_2}p_{\epsilon_3} \\ & \dots p_{\epsilon_{\mu-1}}p_{c_\mu} + (\mu+1)Ip_{\epsilon_1}p_{\epsilon_2}p_{\epsilon_3}\dots p_{\epsilon_\mu}p_{c_1} + (\mu+2)Ip_{\epsilon_1}^2 \\ & p_{\epsilon_2}p_{\epsilon_3}\dots p_{\epsilon_\mu}p_{c_2} + (\mu+3)Ip_{\epsilon_1}^2p_{\epsilon_2}^2p_{\epsilon_3}\dots p_{\epsilon_\mu}p_{c_3} + \dots + \\ & (\mu+\mu)Ip_{\epsilon_1}^2p_{\epsilon_2}^2p_{\epsilon_3}^2\dots p_{\epsilon_{\mu-1}}^2p_{c_\mu} + \dots + (\gamma\mu+1)Ip_{\epsilon_1}^{\gamma}p_{\epsilon_2}^{\gamma} \\ & \dots p_{\epsilon_\mu}^{\gamma}p_{c_1} + (\gamma\mu+2)Ip_{\epsilon_1}^{\gamma}p_{\epsilon_2}^{\gamma}\dots p_{\epsilon_\mu}^{\gamma}p_{\epsilon_1}p_{c_2} + (\gamma\mu+3) \\ & Ip_{\epsilon_1}^{\gamma}p_{\epsilon_2}^{\gamma}\dots p_{\epsilon_\mu}^{\gamma}p_{\epsilon_1}p_{\epsilon_2}p_{c_3} + \dots + (\gamma\mu+\mu)Ip_{\epsilon_1}^{\gamma}p_{\epsilon_2}^{\gamma}\dots p_{\epsilon_\mu}^{\gamma} \\ & p_{\epsilon_1}p_{\epsilon_2}\dots p_{\epsilon_{\mu-1}}p_{c_\mu} + \dots \end{aligned} \quad (24)$$

By rearranging (24), we have

$$\begin{aligned} n_\mu = {} & Ip_{c_1}\Big(1 + (\mu+1)\alpha + (2\mu+1)\alpha^2 + (3\mu+1)\alpha^3 + \\ & \dots\Big) + Ip_{\epsilon_1}p_{c_2}\Big(2 + (\mu+2)\alpha + (2\mu+2)\alpha^2 + (3\mu+2) \\ & \alpha^3 + \dots\Big) + \dots + Ip_{\epsilon_1}p_{\epsilon_2}\dots p_{\epsilon_{J-1}}p_{c_J}\Big(J + (\mu+J)\alpha + \\ & (2\mu+J)\alpha^2 + (3\mu+J)\alpha^3 + \dots\Big) + \dots + Ip_{\epsilon_1}p_{\epsilon_2}\dots \\ & p_{\epsilon_{\mu-1}}p_{c_\mu}\Big(\mu + (\mu+\mu)\alpha + (2\mu+\mu)\alpha^2 + (3\mu+\mu)\alpha^3 + \\ & \dots\Big) \end{aligned} \quad (25)$$

$$\begin{aligned} n_\mu = {} & b_1\Big(1 + (\mu+1)\alpha + (2\mu+1)\alpha^2 + (3\mu+1)\alpha^3 + \\ & \dots\Big) + b_2\Big(2 + (\mu+2)\alpha + (2\mu+2)\alpha^2 + (3\mu+2)\alpha^3 \\ & + \dots\Big) + \dots + b_J\Big(J + (\mu+J)\alpha + (2\mu+J)\alpha^2 + \\ & (3\mu+J)\alpha^3 + \dots\Big) + \dots + b_\mu\Big(\mu + (\mu+\mu)\alpha + \\ & (2\mu+\mu)\alpha^2 + (3\mu+\mu)\alpha^3 + \dots\Big) \end{aligned} \quad (26)$$

where $b_1 = Ip_{c_1}$, $b_2 = Ip_{\epsilon_1}p_{c_2}$ and $b_J = Ip_{\epsilon_1}p_{\epsilon_2}\dots p_{\epsilon_{J-1}}p_{c_J} = k(1+m)\prod_{j=1}^{J} p_{\epsilon_{J-j}}p_{c_J}$. Note that there are μ summation series in (26) and J-th summation series in the above expression is

$$\begin{aligned} n_{J,\mu} = {} & Jb_J + (J+\mu)b_J\alpha + (J+2\mu)b_J\alpha^2 + (J+3\mu) \\ & b_J\alpha^3 + \dots. \end{aligned} \quad (27)$$

Therefor, expected number of information bits need to be transmitted to deliver $k(1+m)$ information bits is

$$n_\mu = \sum_{J=1}^{\mu} n_{J,\mu}. \quad (28)$$

■

Now we are ready to state proposition for throughput of CCSR method with joint detection of μ packet at MAC layer. The following proposition presents throughput of CCSR method:

Proposition 3. *Throughput of CCSR method under maximum number of μ rounds at MAC layer and non-truncated retransmissions at ARQ layer is*

$$\eta_\mu = \frac{(1-\alpha)^2}{(1+m)\sum_{J=1}^{\mu}\prod_{j=1}^{J} p_{\epsilon_{J-j}} p_{c_J}\big(J+(\mu-J)\alpha\big)}, \quad (29)$$

where $\alpha = \prod_{J=1}^{\mu} p_{\epsilon_J}$ *and* $p_{\epsilon_0} = 1$.

Proof: From proposition 2, average number of bits n_μ required to deliver error-free packet to the receiver consists of summation of μ terms. That is,

$$n_\mu = \sum_{J=1}^{\mu} n_{J,\mu} = n_{1,\mu} + n_{2,\mu} + \ldots + n_{\mu,\mu} \quad (30)$$

The J-th summation series is

$$n_{J,\mu} = b_J\Big(J + (\mu+J)\alpha + (2\mu+J)\alpha^2 + (3\mu+J)\alpha^3 + \ldots\Big) \quad (31)$$

$$\begin{aligned} n_{J,\mu}(\alpha-1) &= b_J\Big(-J - \mu\alpha - \mu\alpha^2 - \mu\alpha^3 - \ldots\Big) \\ &= b_J\Big(-J - \mu\alpha(1+\alpha+\alpha^2+\alpha^3+\ldots)\Big) \\ &= b_J\Big(-J - \frac{\mu\alpha}{(1-\alpha)}\Big). \end{aligned} \quad (32)$$

Thus,

$$n_{J,\mu} = b_J \frac{J+(\mu-J)\alpha}{(1-\alpha)^2}. \quad (33)$$

Substituting b_J in (33), we have

$$n_{J,\mu} = (1+m)\prod_{k=1}^{J} p_{\epsilon_{J-k}} p_{c_J} \frac{J+(\mu-J)\alpha}{(1-\alpha)^2}. \quad (34)$$

The average number n_μ of transmitted bits required to deliver single error free bit at receiver under μ transmission rounds at MAC layer of CCSR method is,

$$n_\mu = \sum_{J=1}^{\mu} n_{J,\mu} = (1+m)\sum_{J=1}^{\mu}\prod_{j=1}^{J} p_{\epsilon_{J-j}} p_{c_J} \frac{J+(\mu-J)\alpha}{(1-\alpha)^2} \quad (35)$$

Throughput of CCSR method is

$$\eta_\mu = \frac{1}{n_\mu} = \frac{(1-\alpha)^2}{(1+m)\sum_{J=1}^{\mu}\prod_{j=1}^{J} p_{\epsilon_{J-j}} p_{c_J}\big(J+(\mu-J)\alpha\big)} \quad (36)$$

■

Note that η_μ of CCSR is function of parameter τ that controls the information to be transmitted during selective retransmission. The parameter τ can be optimize to maximize throughput under OFDM signaling. Next, we discuss search for optimal τ for the proposed CCSR method to enhance throughput of an OFDM transceiver.

VI. Throughput Optimization

In this section, we optimize throughput of the proposed selective retransmission method at modulation layer. The amount of information that a receiver requests to the transmitter in the event of a packet failure has direct impact on the throughput of the transceiver. Most of the time, especially in high SNR regime, receiver can recover from bit errors by receiving little more information and employing joint detection. In selective retransmission at modulation level, threshold τ on channel norm of a sub-carrier is measure of channel quality. By choosing proper threshold τ, receiver can request minimum information needed to recover from errors for the failed packet. The threshold τ is function of SNR and modulations such as 4-QAM and 16-QAM. It is clear from (29) that throughput of CCSR method is a function of frame-error rate (FER). Furthermore, FER is not a linear or quadratic function of SNR and parameter τ. Now we write unconstrained optimization problem for throughput η with respect to parameter τ as follows:

$$\tau_o = \arg\max_{\tau} \quad \eta = f(\tau, SNR). \quad (37)$$

Since throughput η is non-convex function in parameter

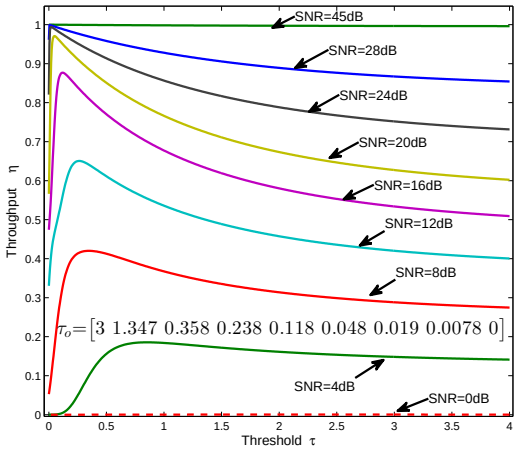

Fig. 3. Analytical throughput (29) vs τ for SNR operating points of CCSR method for $\mu = 2$ transmission rounds.

τ, optimal τ that maximizes throughput η for each SNR can be computed off-line using exhaustive search. Thus, a table of optimal threshold τ which maximizes

throughput for SNR operating points can be generated using throughput expression in (29) for CCSR method. Note that throughput of the proposed CCSR method is function $\eta = f(\tau, SNR)$ given in (29).

In Section VII, we maximize $\eta = f(\tau, SNR)$ with respect to parameter τ. Note that parameter τ appears in probability of frame error p_ϵ, which is function of probability of bit-error presented in (20) Section IV. The optimal τ_o can be computed off-line from throughput lower bound for CCSR using (29). Based on channel condition, amount of information to be transmitted can be controlled using vector τ_o. Figure 3 shows that optimal threshold τ_o for SNR points which maximizes throughput CCSR method for $\mu = 2$. In low SNR regime, throughput η is more sensitive to threshold τ as compared to high SNR regime due to the fact that in high SNR regime, very few errors occur during first transmission resulting into fewer retransmissions.

VII. Simulation

Now we present performance of the proposed CCSR method in comparison with conventional Chase combining methods. In throughput performance, we consider optimized threshold τ_o which controls the amount of information in selective retransmission for OFDM systems. In simulation setup, we consider 4-QAM constellation and OFDM signaling with $N_s = 512$ sub-carriers over 10-tap Rayleigh fading frequency selective channel. Each complex OFDM channel realization has Gaussian distribution with zero-mean and unit variance ($\sigma_h^2 = 1$). We assume block fading channel in quasi-static fashion such that channel remains highly correlated during transmission of one OFDM symbol. First, we present comparison of BER upper bound and BER from Monte Carlo simulation denoted by BER_a and BER_m, respectively, for CCSR method. We also provide throughput results of CCSR method in comparison with conventional Chase combining method. We denote analytical and simulation throughput by η_a and η_m, respectively. In order to maximize throughput, threshold τ on channel norm of OFDM sub-carriers is optimized for each SNR point of CCSR protocol. We compute threshold vector τ_o off-line to maximize throughput of CCSR method from the analytical throughput using (29). We also demonstrate that our proposed CCSR method holds throughput gain with FEC. We consider half-rate LDPC code (648, 324) to evaluate efficacy of CCSR method as compared to conventional CC-HARQ. We denote CCSR method with FEC enabled by CCSR-HARQ in simulation results.

First, we present BER and throughput performance of CCSR method in comparison with conventional CC for $\mu = 1, 2$ and 4 transmission rounds using optimal threshold τ_o without FEC. Note that each SNR point has

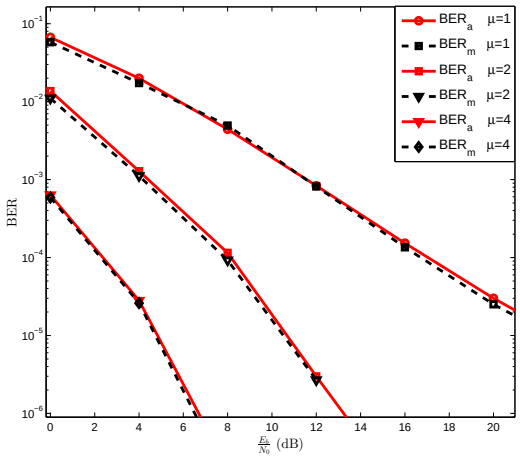

Fig. 4. Monte Carlo simulation Vs BER upper bound (20) of CCSR method for $\mu = 1, 2$ and 4 transmission rounds with optimal threshold τ_o.

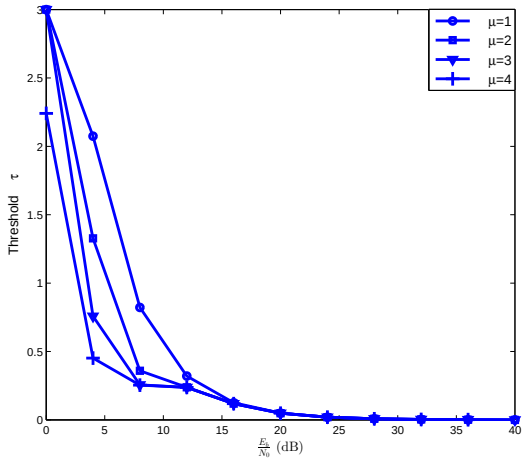

Fig. 5. $\frac{E_b}{N_o}$ vs optimal threshold τ_o which maximizes throughput of CCSR-ARQ method for $\mu = 1, 2, 3$ and 4 transmission rounds.

an associated threshold τ_o which maximizes throughput at that very SNR point. For analytical BER and throughput performance, we use (20) and (29), respectively. We denote CCSR and conventional CC methods without FEC by CCSR-ARQ and CC-ARQ, respectively. Figure 4 provides BER comparison of Monte Carlo simulation and BER upper bound of CCSR-ARQ method for $\mu = 1, 2,$ and 4. Figure 4 reveals that there is marginal gap between analytical and simulation bit-error rates BER_a and BER_m, respectively.

In Figure 5, we present optimal threshold τ_o as a function of SNR. As Figure 5 shows, at $\frac{E_b}{N_o} \geq 8$dB, optimal τ_o for $\mu = 4$ converges to the τ_o for $\mu = 3$. Similarly, at $\frac{E_b}{N_o} \geq 12$dB, optimal τ_o for $\mu = 3$ and

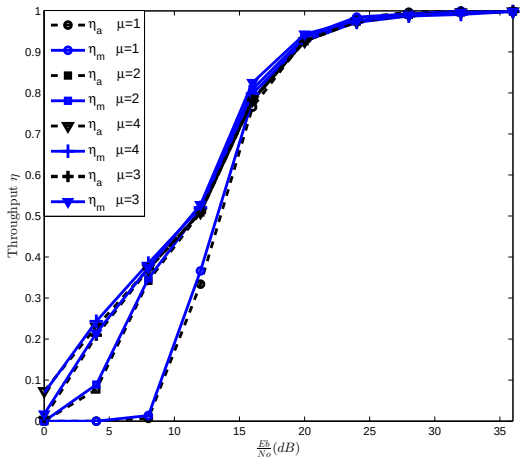

Fig. 6. Monte Carlo simulations Vs analytical throughput using (29) of CCSR-ARQ method for $\mu = 1, 2$ and 4 transmission rounds with optimal threshold τ_o.

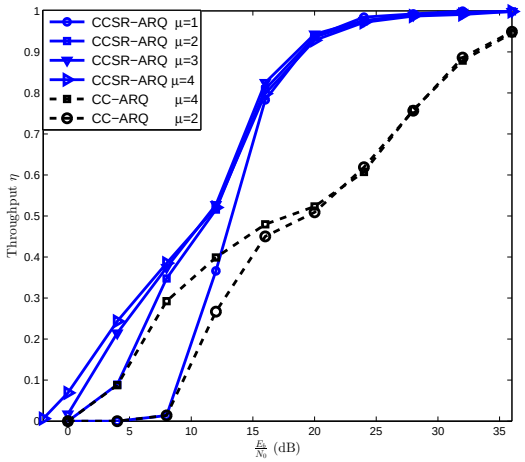

Fig. 7. Throughput comparison of conventional Chase combining CC-ARQ $\mu = 2, 4$ transmission rounds and optimal CCSR-ARQ for $\mu = 1, 2, 3, 4$ transmission rounds using Monte Carlo simulations.

$\mu = 4$ converge to the τ_o for $\mu = 2$. At $\frac{E_b}{N_o} \geq 16$dB, optimal τ_o for $\mu = 2$, $\mu = 3$ and $\mu = 4$ converge to the τ_o for $\mu = 1$. This is due to the fact that as $\frac{E_b}{N_o}$ increases, the probability of entering into next round of transmission (retransmission) at MAC layer decreases. For example, at $\frac{E_b}{N_o} \geq 8$dB, probability that system reaches 4 rounds of transmission is very low and joint detection for $\mu = 4$ converges to the joint detection for $\mu = 3$. We observe similar trend at $\frac{E_b}{N_o} = 12, dB$ and 16dB for $\mu = 3$ and 2, respectively.

Throughput is the key performance metric of a communication system. Now we provide results for tight lower throughput bound and throughput comparison between CCSR-ARQ and CC-ARQ methods. For throughput computation, we use standard definition of throughput of a communication system [2] as $\frac{k}{n}$. In CCSR-ARQ method, threshold vector τ_o in Figure 5 is computed offline using (37) to maximize throughput η. Figure 6 presents comparison of analytical throughput using (29) with Monte Carlo throughput of CCSR-ARQ using optimal τ_o for $\mu = 1, 2$ and 4 transmission rounds. Marginal gap between analytical and simulation throughput demonstrate that (29) provides tight throughput lower bound for CCSR-ARQ for $\mu = 1, 2, 4$. Consistent with Figure 5, at $\frac{E_b}{N_o} \geq 8$dB, throughput for $\mu = 4$ converges to the throughput for $\mu = 3$. Similarly, at $\frac{E_b}{N_o} \geq 12$dB, throughput for $\mu = 4$ converge to the throughput for $\mu = 2$. Also, at $\frac{E_b}{N_o} \geq 16$dB, throughput for $\mu = 2$ and $\mu = 4$ converge to the throughput for $\mu = 1$.

Now we provided throughput comparison between CCSR-ARQ and CC-ARQ methods for different number of transmission rounds. Figure 7 demonstrates that CCSR-ARQ method achieves significant performance gain over conventional CC-ARQ method for $\mu = 1$, 2, 3 and 4 transmission rounds. Note that throughput of CC-ARQ for $\mu = 2$ is similar to that of CCSR for $\mu = 1$ up to $\frac{E_b}{N_o} = 8$dB. This is due to the fact that in low SNR regime, τ_o which maximizes throughput of the system has large value resulting selective retransmission of first round of CCSR into full packet retransmission. Thus, amount of information transmitted in first round of CCSR-ARQ equals amount of information of two rounds of CC-ARQ. For $\frac{E_b}{N_o} \geq 8$dB under $\mu = 1$ for CCSR-ARQ, τ_o decreases as SNR increases and selective retransmission becomes more effective providing larger throughput gain over CC-ARQ. Thus, we observe significant throughput gain of CCSR-ARQ method over CC-ARQ method in moderate and high SNR regime. We notice similar trend when we compare CCSR-ARQ for $\mu = 2$ and CC-ARQ for $\mu = 4$. It is important to note that in low SNR regime, τ_o converges to large values and throughput of CCSR-ARQ converges to that of CC-ARQ. Figure 7 also reveals that large transmission rounds are more effective in low SNR regime.

Aforementioned results demonstrate significant throughput gain of CCSR-ARQ method over CC-ARQ method (without FEC). Now we present BER and throughput performance comparison between CCSR and CC methods with FEC. We denote CCSR and CC methods with FEC by CCSR-HARQ and CC-HARQ, respectively. Figure 8 presents simulation results of BER performance of conventional CC-HARQ and proposed CCSR-HARQ methods with half-rate LDPC (648,324) encoder under OFDM signaling. For BER simulation of CCSR-HARQ method, we use optimal threshold τ_o which maximizes throughput of CCSR-

TABLE I
SNR VS τ_o FOR $\mu = 1, 2, 3$ AND 4

$\frac{E_b}{N_o}/\mu$	-8	-6	-5	-3	-2	0	1	2	3	4	5	6	7	8
1	3	3	3	2.2	1	0.595	0.43	0.301	0.16	0.090	0.030	0.006	0	0
2	3	3	2.82	1.274	0.423	0.9	0.5	0.35	0.2	0.11	0.034	0.004	0	0
3	3	1.9	1.741	0.97	0.4	0	0.7	0.407	0.204	0.118	0.002	0	0	0
4	2.4	1.338	0.949	0.072	0.023	0	0.63	0.36	0.235	0.09	0.0038	0.009	0.0005	0

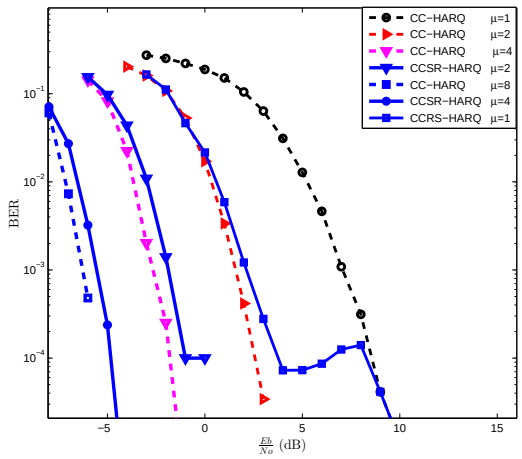

Fig. 8. BER comparison of CCSR-HARQ and conventional CC-HARQ methods for $\mu = 1, 2, 4$ using half rate LDPC code (324, 648) with optimal τ_o.

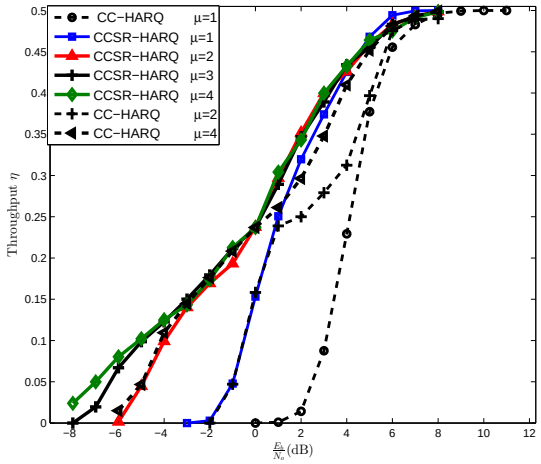

Fig. 9. Throughput comparison CC-HARQ for $\mu = 1, 2, 4$ and CCSR-HARQ for $\mu = 1, 2, 3, 4$ transmission rounds with half rate LDPC code(324,648) using $\tau = \tau_o$.

HARQ method for $\mu = 1, 2,$ and 4. The threshold vectors for $\mu = 1, 2,$ and 4 used in Figure 8 and Figure 7 are given in Table I. Note that CCSR-HARQ and CC-HARQ methods are same for $\tau = 0$. For very large value of threshold $\tau \to \infty$, BER performance of joint detection of CCSR-HARQ for μ transmission rounds is same as that of CC-HARQ for 2μ rounds. In Figure 8, we use optimal threshold τ_o on selective retransmission in PHY which maximizes throughput η. In high SNR regime, single round $\mu = 1$ of CC-HARQ method achieves low probability of error resulting into low packet error rate and low probability of enetering into second round of transmission. In such scenario, optimal threshold $\tau_o \to 0$ and CCSR-HARQ method becomes CC-HARQ method. For $\frac{E_b}{N_o} > 4$dB, $\tau_o \to 0$ and BER curve of CCSR-HARQ for $\mu = 1$ merges with BER of CC-HARQ method. Similarly, we notice that under $\mu = 2$ at $\frac{E_b}{N_o} > -2$dB, optimal threshold τ_o, which maximizes throughput, is very small resulting into merging of BER for $\mu = 2$ and $\mu = 1$. In low SNR regime, BER and throughput of large transmission rounds is better than small transmission rounds. As channel condition improves, the CCSR-HARQ with large μ behaves similar to CCSR-HARQ method with small μ. Furthermore, at a given SNR, there are multiple values of τ which achieve similar throughput. The small threshold on channel norm τ has lower retransmission overhead and results into higher BER. As Figure 8 reveals, BER marginally degrades when $\frac{E_b}{N_o}$ improves from 5 to 8 dB and still provides optimal throughput.

We present throughput of proposed CCSR-HARQ method in comparison with conventional CC-HARQ method in Figure 9. We provide Monte Carlo simulation results of throughput for CCSR-HARQ and CC-HARQ methods for $\mu = 1, 2, 3,$ and 4 transmission rounds using simulation setup of Figure 8. Throughput of CCSR-HARQ for $\mu = 1$ is significantly higher than throughput of CC-HARQ for $\mu = 1$, which demonstrates the efficacy of CCSR method. Also throughput of CCSR-HARQ for $\mu = 1$ and CC-HARQ for $\mu = 2$ are very close when $\frac{E_b}{N_o} \leq 0$dB. However, for $\frac{E_b}{N_o} \geq 0$dB, CCSR-HARQ has higher throughput than CC-HARQ. For larger transmission rounds, CCSR-HARQ is more effective in low SNR regime as shown in Figure 8. Note that impact of selective retransmission in CCSR-HARQ method is not significant for $\mu = 4$ in higher SNR regime due to the fact that CCSR-HARQ has low probability of CRC failure. Figure 9 also reveals that CCSR-HARQ for $\mu = 4$ first converges to CCSR-HARQ for $\mu = 3$ at $\frac{E_b}{N_o} \geq -6$dB. Both curves continue in overlap fashion

and converge to CCSR-HARQ for $\mu = 2$ at $\frac{E_b}{N_o} \geq 0$dB and then $\mu = 2, 3,$ and 4 follows CCSR-HARQ for $\mu = 1$ at $\frac{E_b}{N_o} \geq 3$dB similar to Figure 7.

VIII. Conclusion

We presented bandwidth efficient cross-layer design under OFDM modulation using selective retransmission sub-layer at PHY level. The throughput performance comparison demonstrated that the proposed CCSR method outperforms conventional Chase combing method. In performance analysis, we provided tight BER upper bound and throughput lower bound for the proposed CCSR method. The simulation results suggest that BER and throughput performances from Monte Carlo runs have marginal performance gap from that of BER upper bound and throughput lower bound, respectively. In order to maximize throughput of the CCSR method, we optimized threshold τ which controls amount of information to be retransmitted by embedded selective retransmission at PHY level. The simulation results also demonstrate significant throughput gain of optimized selective retransmission method over conventional Chase combining method with and without channel coding.

References

[1] "Long Term Evolution of the 3GPP Radio Technology," *http:/www.3gpp.org*.

[2] S. Lin and P. S. Yu, "A Hybrid ARQ Scheme with Parity Retransmission for Error Control of Satellite Channels," *IEEE Trans. Commun.*, vol. 30, no. 7, pp. 1701–1719, Jul. 1982.

[3] S. Y. Park and D. Love, "Hybrid ARQ Protocol for Multi-Antenna Multicasting Using a Common Feedback Channel," *IEEE Trans. Commun.*, vol. 59, no. 6, pp. 1530–1542, Jun. 2011.

[4] D. Chase, "Code Combining - A Maximum-Likelihood Decoding Approach for Combining an Arbitrary Number of Noisy Packets," *IEEE Tran. Commun.*, vol. 33, pp. 385–393, May 1985.

[5] C. Shen and M. P. Fitz, "Hybrid ARQ in Multiple-Antenna Slow Fading Channels: Performance Limits and Optimal Linear Dispersion Code Design," *IEEE Trans. Inf. Theory*, vol. 57, no. 9, pp. 5863–5883, Sep. 2011.

[6] P. Wu and N. Jindal, "Coding versus ARQ in Fading Channels: How Reliable Should the PHY Be?" *IEEE Trans. Commun.*, vol. 59, no. 12, pp. 3363–3374, December 2011.

[7] ——, "Performance of Hybrid-ARQ in Block-Fading Channels: A Fixed Outage Probability Analysis," *IEEE Trans. on Comm.*, vol. 58, no. 4, pp. 1129–1141, April 2010.

[8] T. C. E. Larsson, "Optimal Power Allocation for Hybrid ARQ with Chase Combining in i.i.d. Rayleigh Fading Channels," *IEEE Trans. on Commun.*, vol. 61, no. 5, pp. 1835 – 1846, May 2013.

[9] ——, "Outage-Optimal Power Allocation for Hybrid ARQ with Incremental Redundancy," *IEEE Trans. Wireless Commun.*, vol. 10, no. 7, pp. 2069–2074, 2011.

[10] ——, "Adaptive Power Allocation for HARQ with Chase Combining in Correlated Rayleigh Fading Channels," *IEEE Commun. Lett.*, vol. 3, no. 2, pp. 169 – 172, 2014.

[11] Dechene, J. Dan, and A. Shami, "Energy-Aware Resource Allocation Strategies for LTE Uplink with Synchronous HARQ Constraints," *IEEE Trans. Mobile Computing*, vol. 13, no. 2, pp. 422–433, 2014.

[12] B. Makki, G. Amat, and T. Eriksson, "Green Communication via Power-Optimized HARQ Protocols," *IEEE Trans. Veh. Technol.*, vol. 63, no. 1, pp. 161–177, Jan 2014.

[13] M. Zia and Z. Ding, "Joint ARQ Receiver Design for Bandwidth Efficient MIMO Systems," in *Proc. IEEE Global Telecommunication Conference (GLOBECOM'08)*, New Orleans, LO, Dec. 2008, pp. 1–5.

[14] X. Liang, C. M. Zhao, and Z. Ding, "Piggyback Retransmissions over Wireless MIMO Channels: Shared Hybrid-ARQ (SHARQ) for Bandwidth Efficiency," *IEEE Trans. Wireless Commun.*, vol. 12, no. 8, pp. 3770–3782, Aug. 2013.

[15] M. Zia and Z. Ding, "Bandwidth Efficient Variable Rate HARQ Under Orthogonal Space-Time Block Codes," *IEEE Trans. Signal Process.*, vol. 62, no. 3, pp. 3360–3390, Jul. 2014.

[16] R. Jermey and Z. Ding, "Channel Estimation and Equalization Techniques in Downsampled ARQ Systems," *IEEE Trans. Signal Process.*, vol. 55, no. 5, pp. 2251–2262, May. 2007.

[17] S. Alamouti, "A Simple Transmit Diversity Technique for Wireless Communications," *IEEE J. Sel. Areas Commun.*, vol. 16, no. 8, pp. 1451–1458, Oct. 1998.

[18] M.-W. Wu and P.-Y. Kam, "ARQ with Channel Gain Monitoring," *IEEE Trans. Commun.*, vol. 60, no. 11, pp. 3342–3352, Nov. 2012.

[19] M. Zia, H. Mahmood, A. Ahmed, and N. Saqib, "Selective HARQ Transceiver Design for OFDM System," *IEEE Commun. Lett.*, vol. 17, no. 12, pp. 2229 – 2232, Dec. 2013.

[20] T. Kiani, M. Zia, N. Abbas, and H. Mahmood, "Bandwidth-Efficient Selective Retransmission for MIMO-OFDM ," *ETRI*, vol. 37, no. 1, pp. 66–67, 2015.

[21] A. Ahmed, M. Zia, N. Abbas, and H. Mahmood, "Partial Automatic Repeat Request Transceiver for Bandwidth and Power Efficient Multiple-Input Multiple-Output Orthogonal Frequency Division Multiplexing Systems," *IET Communications*, pp. 476–486, Mar. 2015.

[22] M. Zia, "Selective Chase Combining for OSTB Coded MIMO-OFDM System," *International Journal Of Electronics and Communication*, 2015.

[23] A. Larmo, M. Lindstrom, M. Mayer, G. Pelletier, and J. Tornser, "The LTE Link-Layer Design," *IEEE Commun. Mag.*, vol. 47, no. 4, pp. 52 – 59, 2009.

[24] S. Stefania, I. Toufik, and M. Baker, *LTE - The UMTS Long Term Evolution: From Theory to Practice*. Wiley, 2011.

[25] E. G. Larsson and P. Stoica, *Space-Time Block Coding for Wireless Communications*. Cambridge, 2003.

[26] J. Proakis and M. Salehi, *Digital Communications*. McGraw-Hill, 2007.

[27] H. Stark and J. W. Woods, *Probability and Random Processes with Applications to Signal Processing*. Prentice Hall, 2001.

[28] M. Chiani, D. Dardari, and M. K. Simon, "New Exponential Bounds and Approximations for the Computation of Error Probability in Fading Channels," *IEEE Trans. Wireless Commun.*, vol. 2, no. 4, pp. 840–845, July 2003.

[29] S. Lin, D. J. Costello, and M. J. Miller, "Automatic Repeat Request Error Control Schemes," *IEEE Commun. Mag.*, vol. 22, no. 12, pp. 5–14, Dec. 1984.

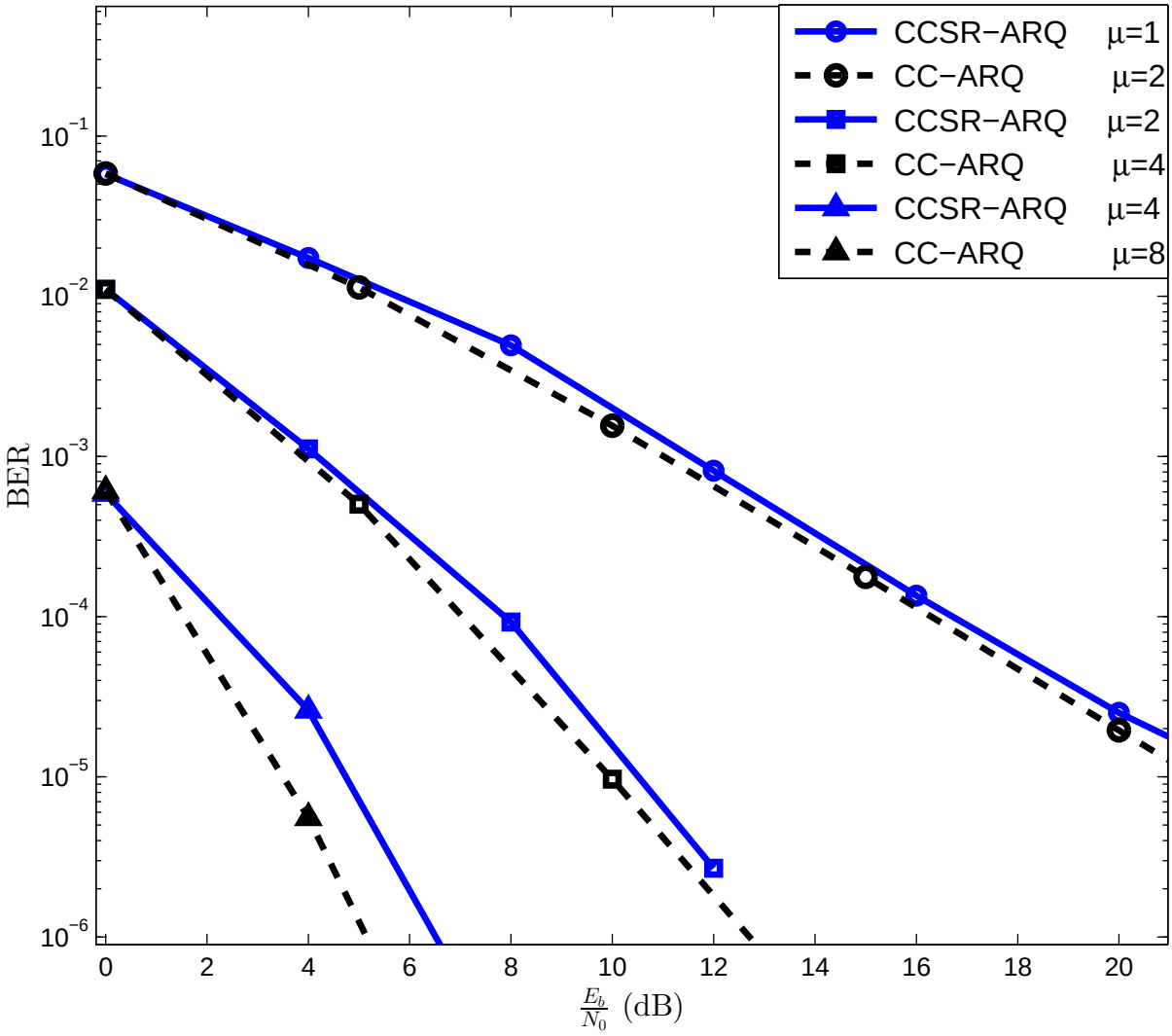
CCSR−ARQ μ=1
CC−ARQ μ=2
CCSR−ARQ μ=2
CC−ARQ μ=4
CCSR−ARQ μ=4
CC−ARQ μ=8
BER
10^{-1}
10^{-2}
10^{-3}
10^{-4}
10^{-5}
10^{-6}
0
2
4
6
8
10
12
14
16
18
20
$\frac{E_b}{N_0}$ (dB)

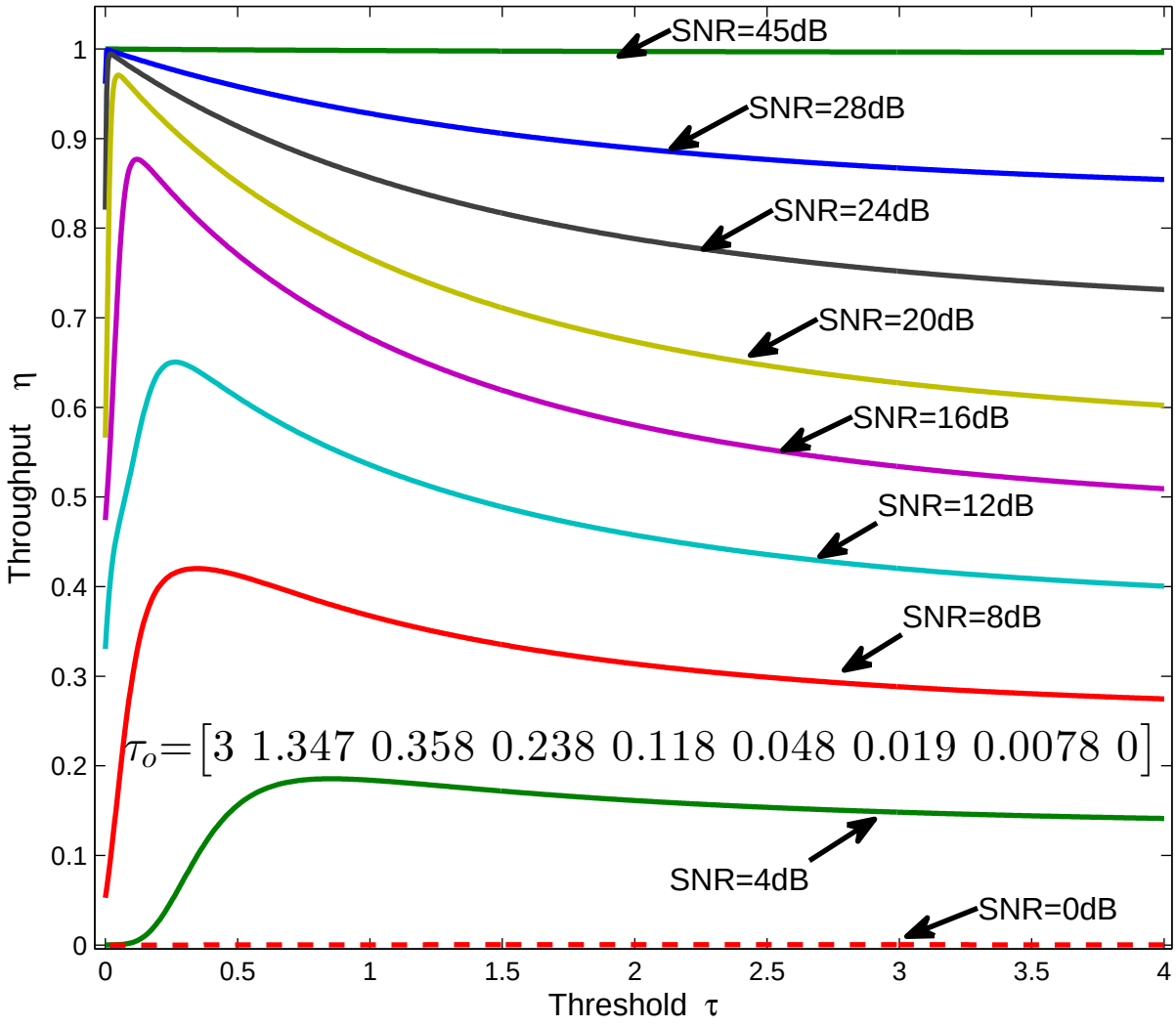
SNR=45dB
SNR=28dB
SNR=24dB
SNR=20dB
SNR=16dB
SNR=12dB
SNR=8dB
SNR=4dB
SNR=0dB
$\tau_o = [3\ 1.347\ 0.358\ 0.238\ 0.118\ 0.048\ 0.019\ 0.0078\ 0]$
Throughput η
Threshold τ
0
0.1
0.2
0.3
0.4
0.5
0.6
0.7
0.8
0.9
1
0
0.5
1
1.5
2
2.5
3
3.5
4